Release of hydrophobic molecules from polymer micelles into cell membranes revealed by Förster resonance energy transfer imaging

Hongtao Chen*†, Sungwon Kim‡, Li Li*†, Shuyi Wang*§, Kinam Park*‡¶, and Ji-Xin Cheng*†¶

*Weldon School of Biomedical Engineering, †Department of Chemistry, and ‡Department of Pharmaceutics and Biomedical Engineering, Purdue University, West Lafayette, IN 47907

Edited by Milan Mrksich, University of Chicago, Chicago, IL, and accepted by the Editorial Board February 21, 2008 (received for review July 27, 2007)

It is generally assumed that polymeric micelles, upon administration into the blood stream, carry drug molecules until they are taken up into cells followed by intracellular release. The current work revisits this conventional wisdom. The study using dual-labeled micelles containing fluorescently labeled copolymers and hydrophobic fluorescent probes entrapped in the polymeric micelle core showed that cellular uptake of hydrophobic probes was much faster than that of labeled copolymers. This result implies that the hydrophobic probes in the core are released from micelles in the extracellular space. Förster resonance energy transfer (FRET) imaging and spectroscopy were used to monitor this process in real time. A FRET pair, $DiIC_{18(3)}$ and $DiOC_{18(3)}$, was loaded into monomethoxy poly(ethylene glycol)-block-poly(D,L-lactic acid) micelles. By monitoring the FRET efficiency, release of the core-loaded probes to model membranes was demonstrated. During administration of polymeric micelles to tumor cells, a decrease of FRET was observed both on the cell membrane and inside of cells, indicating the release of core-loaded probes to the cell membrane before internalization. The decrease of FRET on the plasma membrane was also observed during administration of paclitaxel-loaded micelles. Taken together, our results suggest a membrane-mediated pathway for cellular uptake of hydrophobic molecules preloaded in polymeric micelles. The plasma membrane provides a temporal residence for micelle-released hydrophobic molecules before their delivery to target intracellular destinations. A putative role of the PEG shell in the molecular transport from micelle to membrane is discussed.

Block copolymer micelles (1–4) have attracted growing interest as carriers to deliver drugs including antitumor reagents to the target site via the enhanced permeability and retention effect (5). Hydrophobic molecules, such as paclitaxel (PTX), can be incorporated into the core of polymeric micelles by physical entrapment. The core composed of hydrophobic chains is expected to regulate the retention and the release of loaded drug molecules on an appropriate time scale (6–8). With micelle-based drug formulations reaching clinical trials (9, 10), the impetus for understanding the pathways involved in micellar drug delivery starts to emerge. It is thought that intact polymeric micelles are taken into cells, followed by intracellular release of drug molecules (8). Kabanov's group (11) reported that pluronic copolymer micelles could be internalized by an endocytic pathway and increase drug absorption by inhibition of P-glycoprotein drug efflux system in cancer cells. Allen *et al.* (12) suggested that poly(ethylene oxide)-poly(ε-caprolactone) (PEO-PCL) micelles enter PC12 cells via endocytosis. To directly monitor the micelles, Luo *et al.* (13) and Savic *et al.* (14) chemically conjugated a rhodamine molecule to the end of the PCL block and investigated the internalization of PEO-PCL micelles into P19 and PC12 cells. In their study, micelles were reported to enter the cell by endocytosis after nonspecific association with the cell membrane (8). It was argued later that these observations were not indicative of the intracellular distribution of the nonionic micelles because the modification with a cationic marker could change the property of copolymer (15). At present, the pathway for cellular internalization of polymeric micelles and incorporated drug molecules remains unclear.

In this study, we investigated the cellular uptake of hydrophobic molecules preloaded in PEG-polyester micelles. Monomethoxy poly(ethylene glycol)-b-poly(D,L-lactic acid) (PEG-PDLLA) micelles were studied because they have been widely used as carriers of PTX (10). PEG-PDLLA was labeled with fluorescein isothiocyanate (FITC) to monitor the micelle itself, and $DiIC_{18(3)}$, a hydrophobic fluorescence probe, was used to represent a hydrophobic drug loaded in the micelle cores. It was found that cellular uptake of $DiIC_{18(3)}$ was much faster than that of FITC-labeled copolymers, indicating two separate cell entry pathways for $DiIC_{18(3)}$ and the copolymers. To clarify this process, we used Förster resonance energy transfer (FRET) to monitor the release of core-loaded molecules from micelles in real time. A FRET pair of hydrophobic dyes, $DiIC_{18(3)}$ as acceptor and $DiOC_{18(3)}$ as donor (referred to as DiI and DiO, respectively), was physically loaded into the micelle cores. FRET between DiO and DiI was recently used to detect plasma membrane heterogeneity (16). In our case, FRET occurred in intact micelles because of intimate DiI/DiO contacts in the cores, whereas the decomposition of micelles by acetone or the release of DiI and DiO from micelles caused a loss of the FRET effect. The results of this study show that during micelle–membrane interactions, the core-loaded molecules are effectively transferred to the plasma membrane, from which they can either be endocytosed or diffuse to the targets; i.e., specific intracellular structures.

Results

Dual-labeled PEG-PDLLA micelles (Fig. 1*A Inset*; containing 10% FITC-PEG-PDLLA and 0.15% DiI) with an average diameter of 52 nm were prepared by dialysis at the 2 mg/ml administration dose and used for the study of cellular uptake of copolymers and core-loaded hydrophobic molecules. KB cells were imaged after a 24-h incubation with 0.2 mg/ml dual-labeled micelles at 37°C. Almost no FITC-labeled copolymers (green in Fig. 1*A*) were found inside of cells, whereas the DiI (red in Fig. 1*B*) initially loaded in the micelle core was significantly internalized into cells. Moreover, the DiI delivered by micelles (Fig.

Author contributions: K.P. and J.-X.C. designed research; H.C., S.K., L.L., and S.W. performed research; and H.C. wrote the paper.

The authors declare no conflict of interest.

This article is a PNAS Direct Submission. M.M. is a guest editor invited by the Editorial Board.

§Permanent address: College of Medical Device Engineering, University of Shanghai for Science and Technology, Shanghai 200093, China.

¶To whom correspondence may be addressed. E-mail: kpark@purdue.edu or jcheng@purdue.edu.

This article contains supporting information online at www.pnas.org/cgi/content/full/0707046105/DCSupplemental.

www.pnas.org/cgi/doi/10.1073/pnas.0707046105

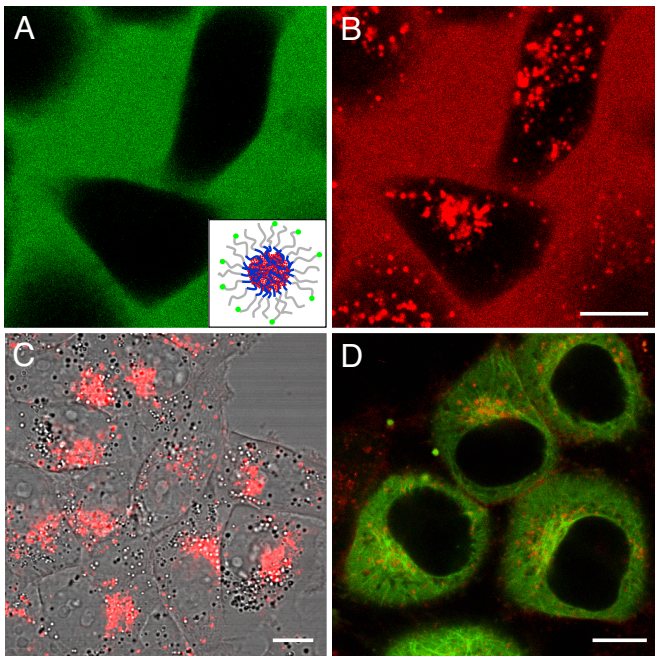

Fig. 1. Cellular internalization of fluorescently labeled micelles and core-loaded hydrophobic probes inspected by confocal fluorescence microscopy. (*A* and *B*) KB cells treated with 0.2 mg/ml dual-labeled micelles for 24 h. The green color represents the FITC signal from labeled micelles, and the red color represents the DiI signal. (*Inset*) Diagram of a micelle labeled with FITC and loaded with DiI. (*C*) KB cells incubated with free DiI in DMSO at the final concentration of 0.1 μg/ml for 24 h. (*D*) HeLa cells incubated with 0.2 mg/ml micelles (physically loaded with 0.15% DiI) for 2 h. DiI was accumulated in the microtubule organizing center area. (Scale bars: 10 μm.)

1*B*) and the free DiI delivered by DMSO (Fig. 1*C*) exhibited the same pattern of perinuclear accumulation. These observations imply that DiI escaped from micelles and entered the cells separately. The intracellular distribution of DiI was further examined by using HeLa cells stably transfected with GFP-tubulin. After a 2-h incubation at 37°C with 0.2 mg/ml micelles loaded with 0.15% DiI, vesicles containing DiI were found to be accumulated in the microtubule organizing center area (Fig. 1*D*), indicative of endosomal localization of DiI. The same pattern was observed in HeLa cells incubated with free DiI (data not shown). Taken together, these results suggest that DiI could escape from the micelles and internalize into cells via endocytosis.

To monitor the release of the core-loaded molecules in real time, we physically loaded a FRET pair into micelles (referred to as FRET micelles), as shown in Fig. 2*A*. The FRET micelles containing 0.75% DiI and 0.75% DiO were prepared by dialysis at an initial concentration of 2 mg/ml copolymer. The micelles were stable for >3 months with an average diameter of 60 nm measured by dynamic light scattering (DLS) and a zeta potential of −6.19 (±0.06) mV. To verify the occurrence of FRET, fluorescence spectra of 0.2 mg/ml micelles in deionized water or acetone were measured on a spectrometer with 484-nm excitation. For micelles in deionized water, a strong DiI signal was observed (red curve in Fig. 2*B*) due to the close proximity of DiI and DiO in the micelle core, with a FRET ratio $I_R/(I_G + I_R)$ of 0.90, where I_R and I_G are fluorescence intensities at 565 nm and 501 nm, respectively. After micelle decomposition by acetone, FRET disappeared (green curve in Fig. 2*B*) because DiI and DiO could not be closely retained anymore, resulting in a FRET ratio $I_R/(I_G + I_R)$ of 0.17. Fluorescence spectra of micelles loaded with 0.75% DiI alone or 0.75% DiO alone [supporting

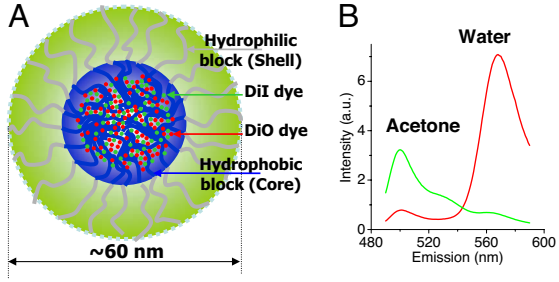

Fig. 2. PEG-PDLLA FRET micelles. (*A*) Diagram of a FRET micelle prepared with 0.75% DiO and 0.75% DiI at 2 mg/ml polymer concentration. (*B*) Spectra of micelles diluted by 10× water (red curve) and 10× acetone (green curve), respectively.

information (SI) Fig. S1] excited at 484 nm show that cross-talk and direct acceptor excitation are minor effects in comparison with the FRET inside of the micelle core. We have also determined the homo-FRET by measuring the fluorescence anisotropy from micelles loaded with different amounts of DiI or DiO. The result shows self-quenching of DiO and DiI fluorescence increased with the loading concentration (Fig. S2). With these characterizations, it is possible to monitor the liberation of DiI and DiO from micelles or decomposition of micelles by measuring the FRET effects, as described below.

The FRET micelles were first applied to model membranes to examine the release of the core-loaded hydrophobic probes to lipid bilayers. Homogeneous supported bilayer and small unilamellar vesicle (SUV) samples were prepared as described in ref. 17. A supported bilayer composed of dioleoyl phosphatidylcholine (DOPC) was incubated with 0.2 mg/ml FRET micelles at room temperature for 2 h. The bilayer was then washed with deionized water. Two-color fluorescence imaging was performed with 488-nm excitation on a confocal microscope. Both DiO fluorescence (Fig. 3*A*) and DiI fluorescence (Fig. 3*B*) from the bilayer were observed, with a ratio $I_{DiI}/(I_{DiI} + I_{DiO})$ of 0.37. As a control, 0.2 mg/ml FRET micelles in water were also imaged (Fig. 3 *C* and *D*), and a higher ratio $I_{DiI}/(I_{DiI} + I_{DiO})$ of 0.89 was obtained. These results indicate that DiI and DiO were effectively relocated to the lipid bilayer during the micelle–bilayer interaction.

To monitor the dynamics of such transfer, 5 μl of 2 mg/ml FRET micelles were mixed with 2 ml of DOPC SUV solution (4 mM), resulting in a final micelle concentration of 5 μg/ml. The time-resolved spectra measured every 15 min over a 2-h period are shown in Fig. 3*E*. A burst decrease of DiI signal was found in the first 15 min, followed by very small changes. On the contrary, the DiO signal increased gradually during the 2-h period. The increase of DiO intensity and decrease of DiI intensity indicate a reduction of FRET due to release of the probes from micelles. To explain the different patterns of intensity change between DiI and DiO, a time-resolved fluorescence study of micelles loaded with DiI or DiO alone was carried out. The results are shown in Fig. 3 *F* and *G*. For DiO-loaded micelles at 484-nm excitation, mixing with SUVs caused a decrease of DiO fluorescence in the first 15 min, followed by a substantial increase. The initial stage (i.e., within 15 min) can be attributed to the burst release of probes located at the hydrophobic-hydrophilic interface inside of the micelle (18, 19), in which the intensity drop shows the effect of local environment (micelle versus lipid membrane) on the probe fluorescence. The later stage can be attributed to the release of high-density probes from the micelle core. Because the release also reduced the probe density inside of the core, the self-quench was effectively attenuated, resulting in an increase of total DiO intensity as shown in Fig. 3*G*. The DiI-loaded micelles displayed the similar

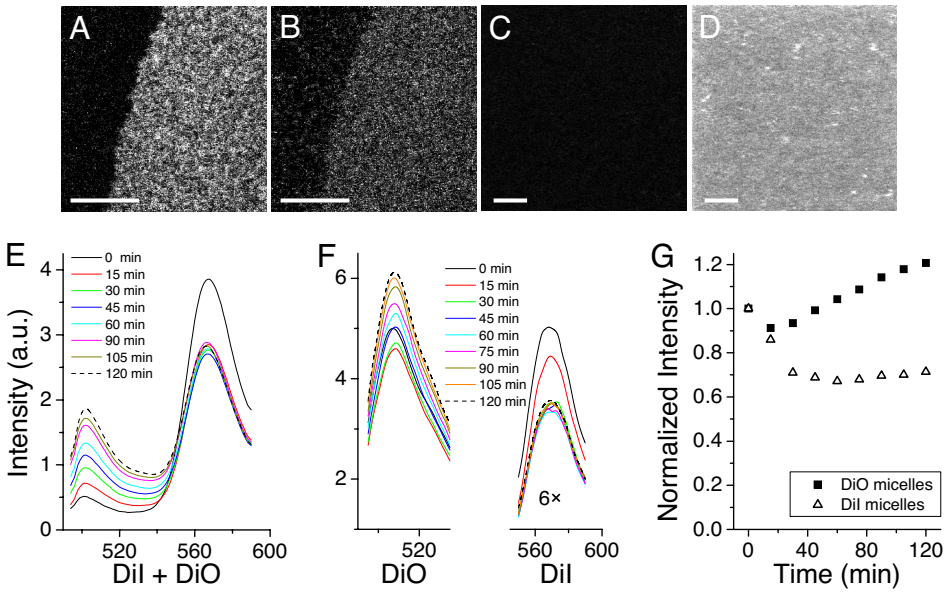

Fig. 3. Transfer of core-loaded probes to model membranes. (*A* and *B*) Fluorescence images of core-loaded DiO (*A*) and DiI (*B*) transferred to the DOPC supported bilayer. $I_{DiI}/(I_{DiI} + I_{DiO}) = 0.37$. (*C* and *D*) Fluorescence images of DiO (*C*) and DiI (*D*) FRET micelles in water with 0.2 mg/ml concentration. $I_{DiI}/(I_{DiI} + I_{DiO}) = 0.89$. (Scale bars: 5 μm.) (*E*) Time-resolved spectra of 5-μl FRET micelles mixed with 2 ml of SUV solution (DOPC, 4 mM). (*F*) Time-resolved spectra of DiI- and DiO-loaded micelles mixed with the DOPC SUV solution under the same condition. The excitation was 484 nm. To ensure the same probe density in the core, the micelles were loaded with 1.5% DiI or 1.5% DiO alone. The DiI fluorescence was magnified by six times for easy comparison. (*G*) Change of total DiO and DiI fluorescence intensity after mixing the DiO- and DiI-loaded micelles with the DOPC SUV solution. The intensity at each time point was normalized by the intensity at 0 min.

behavior in the SUV solution, but the fluorescence level was much lower than for DiO-loaded micelles at 484-nm excitation. The DiI fluorescence is magnified by six times in Fig. 3*F* for easy comparison. The change of total DiO or DiI fluorescence after mixing micelles with SUV is summarized in Fig. 3*G*, where the intensity at each time point is normalized by the intensity at 0 min. These results provide insight into the FRET measurement shown in Fig. 3*E*. During the release of the probes, both reduction of FRET from DiO to DiI and relaxation of DiO self-quench increased the DiO signal. For DiI fluorescence, the initial burst release of probes located at the edge of the core caused a reduction of FRET, which effectively decreased the DiI signal. After that, the release of probes from the micelle core not only reduced the energy transfer from DiO to DiI, but also diminished the DiI self-quench (i.e., homo-FRET, as shown in Fig. S2). The reduction of homo-FRET, together with the cross-talk of increased DiO signal, could counterbalance the reduction of hetero-FRET, leading to a small change of DiI intensity, as shown in Fig. 3*E*.

The above model membrane studies suggest that hydrophobic molecules could be efficiently transferred to lipid bilayers within minutes, where the lipid bilayer served as a sink to accommodate these molecules preloaded into the core of micelles. We have further explored the effect of the membrane–micelle interaction on micelle-based drug delivery to tumor cells. By incubating KB cells with 0.2 mg/ml FRET micelles at 37°C for 2 h, we observed a strong DiO (green in Fig. 4*A*) signal on the plasma membrane and an overlay of DiO and DiI (yellow in Fig. 4*A*) inside of cells. The presence of DiO but lack of DiI fluorescence from the plasma membrane indicated a release of the probes from the micelle core to the membrane where the FRET effect was significantly diminished. After the internalization, DiO and DiI could be concentrated in endocytic vesicles as a result of intracellular sorting, resulting in partial recovery of FRET and an increase of DiI intensity accordingly. The FRET efficiencies were quantified by the spectra recorded from a fluorescent area inside of cells and in the extracellular space (Fig. 4*B*). Whereas a high FRET ratio (0.73) was retained outside of the cells (green curve), a lower FRET ratio (0.33) was obtained inside of the cells (red curve). In a dose-dependent study, KB cells were incubated with 0.1 and 0.02 mg/ml FRET micelles for 0.5 and 2 h before imaging. It was found that DiI and DiO were released to the

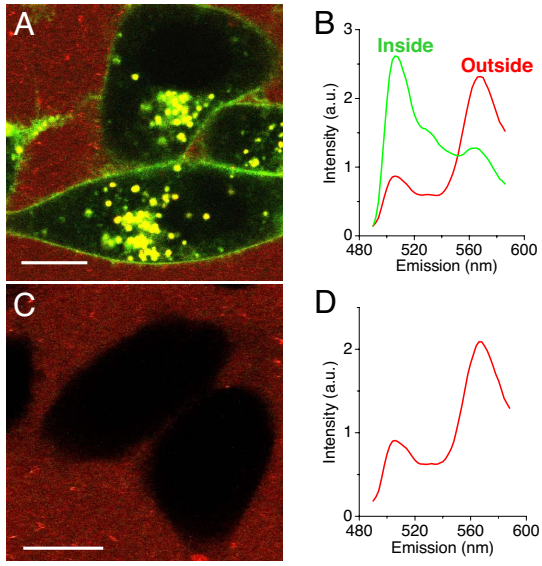

Fig. 4. Transfer of core-loaded probes to plasma membrane. (*A*) Confocal fluorescence image of KB cells incubated with 0.2 mg/ml FRET micelles. After 2 h incubation, image shows that FRET disappeared on cell surface and in intracellular space. (Scale bars: 10 μm.) (*B*) Spectra measured outside (green) and inside (red) of cells. $I_R/(I_G + I_R)$ were 0.73 and 0.33, respectively. The green curve was rescaled to match the red curve, because accumulation of DiI and DiO inside of cells led to a much stronger signal inside of cells than outside of cells. (*C*) Confocal fluorescence image of KB cells incubated with FRET micelles at 4°C for 2 h. (*D*) Spectrum of the extracellular space after 4°C incubation. $I_R/(I_G + I_R)$ was 0.70.

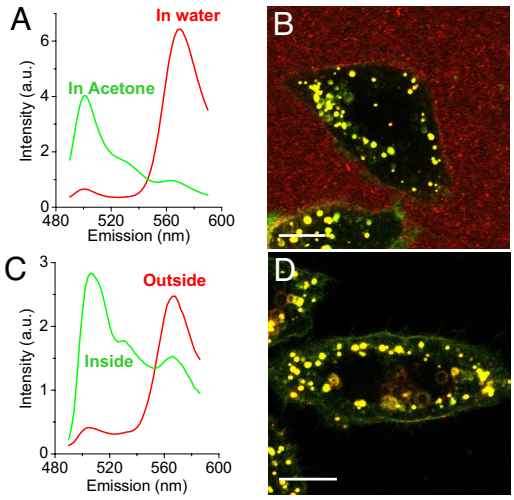

Fig. 5. Transfer of core-loaded molecules to cells from PTX-containing FRET micelles. (*A*) Emission spectra of micelles in water and in acetone with 10× dilution. (*B*) KB cells treated with 0.2 mg/ml micelles for 2 h. High FRET was observed outside of cells, and low FRET was observed on plasma membrane and inside of cells. (Scale bars: 10 μm.) (*C*) Spectra measured outside (green) and inside (red) of cells. $I_R/(I_G + I_R)$ are 0.85 and 0.33, respectively. (*D*) KB cells after two washes. DiO signal (green) was found on the cell membrane.

plasma membrane at all micelle concentrations (Fig. S3). Together with the model membrane studies shown in Fig. 3, our results indicate an effective release of DiI and DiO to the plasma membrane and internalization of those molecules afterward. To examine the pathway involved in the internalization of DiI and DiO, cytochalasin D, which disrupts the actin filaments, and sodium azide, which depletes the energy required for endocytosis, were used to suppress endocytosis. As shown in Fig. S4, with cytochalasin D or NaN_3 treatment, the transfer of probes from micelle core to plasma membrane was observed. However, no DiO or DiI signal was detected inside of the cells. These results confirm that DiI and DiO entered the cells via endocytosis.

A temperature-control experiment was carried out to further examine the transfer of DiI and DiO from micelles to cell membranes. After a 2-h incubation at 4°C, no DiI or DiO fluorescent intensity was probed at the plasma membrane (Fig. 4*C*). Moreover, the spectrum of the extracellular micelles (Fig. 4*D*) was similar to that in Fig. 4*B*. These results confirm the integrity of micelles with DiI and DiO molecules in the cores. Because the glass transition temperature of PDLLA ranges from 26°C to 39°C depending on the molecular weight (20, 21), it is reasonable to assume that transfer of DiI/DiO from the micelle core to the membrane can be inhibited at 4°C.

The same FRET method was used to evaluate PTX-loaded micelles. PTX is a hydrophobic molecule with broad anticancer activity because of its capability of stabilizing the microtubule network (22). Despite the wide use of polymeric micelles for delivery of PTX to cells (23, 24), the pathway is not yet clarified. Previous studies suggested that membranes could provide a lipid sink for limited amount of PTX (25, 26). Thus, PTX could be transferred from the micelles into the plasma membrane and then diffused to microtubules. To examine such a pathway, we prepared PTX-loaded FRET micelles by coloading 10% PTX, 0.75% DiO, and 0.75% DiI during dialysis. These micelles had an average diameter of 80 nm measured by DLS and a zeta potential of −4.68 (±0.74) mV. The fluorescence spectra of micelles in water and acetone shown in Fig. 5*A* demonstrated that FRET occurred in the PTX-loaded FRET micelles. When incubating KB cells with 0.2 mg/ml micelles at 37°C for 2 h, a strong DiI signal (red in Fig. 5*B*) was observed outside of the cells, whereas an overlay of DiO and DiI (yellow in Fig. 5*B*) was found inside of the cells. This observation indicates the release of DiI and DiO. The microspectroscopy analysis in Fig. 5*C* confirms a strong FRET in the extracellular space and a weak FRET inside of the cells. The fluorescent endosomes were scattered into the whole cytosol (Fig. 5*B* and Fig. S5), in contrast to the perinuclear accumulation in cells administrated with normal FRET micelle (Fig. 4*A*). Such difference proves the release of PTX molecules that stabilized the microtubule and hence changed the distribution of endosomes associated with microtubules (27). Importantly, after washing with fresh medium to remove the micelles, the DiO signal was observed on the plasma membrane of the cell (Fig. 5*D*), indicating the release of fluorescent probes and presumably PTX to the plasma membrane before their internalization. An MTT assay was carried out to characterize the cytotoxicity of various PEG-PDLLA micelles under the current study. The results (Fig. S6) demonstrate no cytotoxicity of the FRET micelles and unloaded micelles. However, the PTX coloaded FRET micelles significantly reduced the absorbance at 540 nm, indicating an effective delivery of PTX to cells during the 2-h incubation.

With high hydrophobicity, PCL was used to increase the retention of the hydrophobic molecules in the core of micelles (28, 29). To study the release of DiI and DiO from PEG-PCL micelles, we prepared FRET micelles using PEG-PCL (5,000:2,000) at 2 mg/ml loaded with 0.75% DiI and 0.75% DiO. By incubating 0.2 mg/ml micelles with KB cells at 37°C for 2 h, we observed a strong DiI signal (red in Fig. 6*A*) in the extracellular space, a strong DiO signal (green in Fig. 6*A*) on the plasma membrane, and an overlay of DiO and DiI (yellow in Fig. 6*A*) in the intracellular space. Microspectroscopic analysis

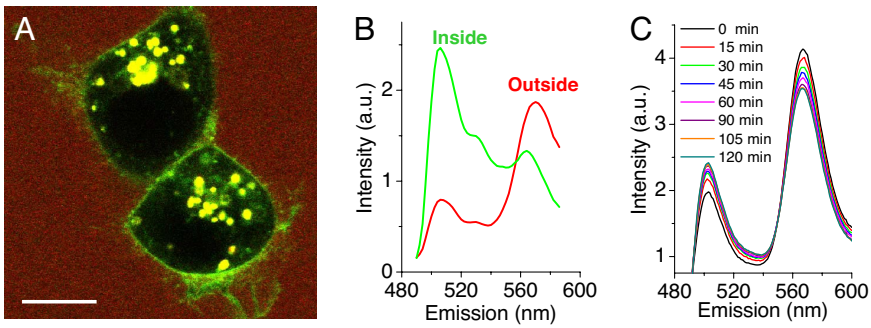

Fig. 6. Uncontrolled release of FRET probes from PEG-PCL micelles. (*A*) Confocal fluorescence image of KB cells incubated with 0.2 mg/ml FRET micelles. (Scale bar: 10 μm.) (*B*) Spectra of FRET micelles in the extracellular space (red) and intracellular space (green). (*C*) Time-resolved spectra of 5-μl FRET micelles mixed with 2 ml of SUV solution (DOPC, 4 mM).

shown in Fig. 6*B* confirms a strong FRET outside of the cell (red curve) and a weak FRET inside of the cell (green curve), consistent with the case of PEG-PDLLA FRET micelles shown in Fig. 4 *A* and *B*. These results suggest that release of hydrophobic molecules from self-assembled PEG-PCL micelles to cells occurred in a way similar to that for PEG-PDLLA micelles. We also used DOPC SUV solution to monitor the dynamics of DiI and DiO release from micelles to lipid bilayers. The time-resolved emission spectra measured for a 2-h period with 5 μg/ml micelles are shown in Fig. 6*C*. A gradual increase of the DiO fluorescence and simultaneous diminution of the DiI fluorescence were observed. Accordingly, the FRET ratio decreased from 0.68 at 0 h to 0.59 at 2 h. It is notable that no burst release was observed, implying an enhanced retention of hydrophobic molecules in the PCL core.

Discussion

Understanding the mechanisms underlying the drug delivery by micelles to cellular and subcellular targets is critical for the design of micelles as effective drug carriers (30, 31). Although internalization of micelles was reported previously (14, 32, 33), the current work showed that internalization of micelles was much slower than that of core-loaded hydrophobic molecules (Fig. 1 *A* and *B*). By FRET experiments in model membranes (Fig. 3) and in cells (Figs. 4–6), we found that core-loaded DiI and DiO were released to plasma membranes and internalized by cells afterward. These results show that micelles exhibit membrane-mediated transportation of hydrophobic agents to cells.

The dynamic instability of polymeric micelles provides a possible mechanism for the release of hydrophobic molecules from micelle core to lipid bilayers. However, it was shown that dynamic exchange between micelles requires days (34, 35), much more time than the release observed in our experiments. We propose that the fast release is facilitated by the PEG shell in micelles. PEG-induced fusion of model membranes has been well studied (36, 37). It is hypothesized that PEG can force very close contact between vesicle membranes by lowering the activity of water adjacent to the membrane (38). In addition, PEG can dehydrate the lipid bilayer, leading to the formation of nonlamellar structures, raising the gel-to-fluid phase transition temperature (39, 40), and enhancing membrane permeability (41). It was also reported that lipid-soluble probes on the membrane of labeled cells could diffuse to the membrane of unlabeled cells at a high PEG concentration, indicating a PEG bridge between the phospholipid membranes of adjacent cells (42). In our study, although the overall PEG concentration in the solution is low with 0.1 mg/ml, the PEG density at the micelle surface is locally high because of the self-assembly of copolymers—e.g., assuming 1,000 copolymer molecules in a micelle of 60 nm diameter, the average PEG density would be 73 mg/ml. The high-density PEG could bridge the transfer of hydrophobic molecules from micelle core to lipid membrane.

Our observation of the fast release of drug molecules from micelles to lipid sinks explains the previous study by Burt *et al.* (43), who observed that PTX rapidly dissociated from the micelle in the blood. Such dissociation is likely due to the transfer of PTX to the abundant lipid components and carriers in the blood. This uncontrolled drug release limits the applications of micelles as a drug delivery system. Although the targeting efficiency can be enhanced by functionalizing micelles with ligands that have selective affinity for recognizing and interacting with a specific cell, tissue, or organ in the body (44), it cannot avoid the drug release during *in vivo* transportation. Shell-cross-linked biodegradable micelles would be a practical method for overcoming the uncontrolled release of drug to lipid environment. Physically incorporated drug molecules can be shielded tightly by the cross-linked corona, and biodegradable cross-linking can allow the release of the drug from micelles in a controlled manner.

Materials and Methods

Materials. Unless stated otherwise, all of the reagents and solvents were used as originally procured. α-Amino-methoxy PEG (MPEG-NH_2; MW 5,000) was purchased from Nektar. D,L-lactide (LA), 10-hydroxydecanoic acid (HDA), dicyclohexyl carbodiimide (DCC), *N*-hydroxysuccinimide (NHS), triethylamine (TEA), stannous 2-ethyl-hexanoate [$Sn(Oct)_2$], dibutyltin dilaurate (DBDL), *bis*-amino-PEG (H_2N-PEG-NH_2), cytochalasin D, and sodium azide were purchased from Sigma–Aldrich. PTX was supplied by Samyang Genex. DiI, DiO, FITC, and the MTT assay kit were purchased from Invitrogen. DOPC was purchased from Avanti Polar Lipids.

Polymer Synthesis and Micelle Preparation. Details on synthesis of copolymers and their fluorescent conjugates can be found in *SI Methods*. Dual-labeled PEG-PDLLA micelles were prepared by the precipitation and membrane dialysis method. Block copolymers (90 mg of PEG-PDLLA, 10 mg of FITC-PEG-PDLLA) were dissolved in 5 ml of acetone with 0.15 mg of DiI. After stirring for 30 min, the solution was dropped to 50 ml of deionized water at 2 ml/min speed and followed by 3 h of stirring to vaporize acetone. Block copolymer aqueous solution was then dialyzed against 2 liters of deionized water (Spectra/Por MWCO 3500) for 2 days. Water was changed after 1 day. Finally, the solution was filtered through a 0.45-μm filter to remove undesirable aggregates, and stored at 4°C. The administration concentration of 2 mg/ml was calculated according to the copolymer and deionized water used.

A similar procedure was used to prepare PEG-PDLLA micelles with 0.15% DiI, PEG-PDLLA FRET micelles, PTX-loaded FRET micelles, and PEG-PCL (5,000:2,000) FRET micelles. In the FRET micelle preparation, DiI and DiO were mixed with 100 mg of copolymer at a 0.75% weight ratio in 5 ml of acetone solution. In the PTX-loaded FRET micelle preparation, 10 mg of PTX was supplied to this 5-ml acetone solution.

The average size of block copolymer micelles were measured by DLS at 23°C. DLS measurement was carried out using a DynaPro99 molecular-sizing instrument equipped with a microsampler (Protein Solutions). The intensity autocorrelation was measured at a scattering angle of 90°. The program CORAN was used for data analysis to obtain the size distribution of micelles. The zeta potential was measured by using the ZetaPALS (Brookhaven Instruments). The anisotropy was measured by using the SpectraMax M5 (Molecular Devices).

Cell Culture. KB cells, a tumor cell line, were obtained from American Type Culture Collection (ATCC CCL-17). A GFP-tubulin stably transfected HeLa was a kind gift from Xiaoqi Liu (Purdue University). Cells were cultured at 37°C in a humidified atmosphere containing 5% CO_2 and grown continuously in RPMI medium 1640 supplemented with 10% FBS, 100 unit/ml penicillin, and 100 μg/ml streptomycin. Coverslip-bottomed Petri dishes (MatTek) were used for high-resolution imaging. Before each experiment, 6×10^4 cells in 1 ml of growth medium were deposited into a Petri dish and incubated for 3–4 days to encourage adherence and cell confluence. The cells in 0.9 ml of culture medium containing 10% FBS were supplemented with 100 μl of micelles and incubated at 37°C or 4°C for the desired lengths of time before imaging.

FRET Imaging, Microspectroscopy, and Spectroscopy. Imaging was performed by using a FV1000 confocal system (Olympus). A 543-nm HeNe laser was used to excite DiI. An Ar^+ laser was used to excite DiO, FITC, and GFP. A 405/488 nm excitation dichroic mirror was used to reflect the 488-nm beam to the sample. FRET images were acquired with 488-nm excitation, spectral filter of 555–655 nm for DiI detection, and spectral filter of 500–530 nm for DiO detection. All of the images were obtained and processed with FluoView software (Olympus). Raw images in OIB format were converted to 8-bit tiff files with pseudocolors for display. Only brightness and contrast were optimized, and no other image processing was used. Microspectroscopy at pixels of interest was carried out by using a spectral detector, with emission scan from 490 to 590 nm. Fluorescence spectra of FRET micelles were measured by using the AMINCO-Bowman series 2 luminescence spectrometer (SLM Aminco Bowman) with 484-nm excitation and emission scan from 490 to 590 nm.

ACKNOWLEDGMENTS. This work was supported by a seed grant from the Purdue University Oncological Sciences Center, National Science Foundation Grant 0416785-MCB (to J.-X.C.), and National Institutes of Health Grants GM065284 and HL078715 (to K.P.).

1. Kataoka K, Kwon GS, Yokoyama M, Okano T, Sakurai Y (1993) Block copolymer micelles as vehicles for drug delivery. *J Controlled Release* 24:119–132.
2. Kwon GS, Kataoka K (1995) Block copolymer micelles as long-circulating drug vehicles. *Adv Drug Delivery Rev* 16:295–309.
3. Moghimi SM, Hunter AC, Murray JC (2001) Long-circulating and target-specific nanoparticles: Theory to practice. *Pharmacol Rev* 53:283–318.
4. Gaucher G, *et al.* (2005) Block copolymer micelles: Preparation, characterization and application in drug delivery. *J Controlled Release* 109:169–188.
5. Maeda H, Wu J, Sawa T, Matsumura Y, Hori K (2000) Tumor vascular permeability and the EPR effect in macromolecular therapeutics: A review. *J Controlled Release* 65:271–284.
6. Washington C (1990) Drug release from microdisperse systems: A critical review. *Int J Pharm* 58:1–12.
7. Lim Soo P, Luo L, Maysinger D, Eisenberg A (2002) Incorporation and release of hydrophobic probes in biocompatible polycaprolactone-block-poly(ethylene oxide) micelles: Implications for drug delivery. *Langmuir* 18:9996–10004.
8. Hubbell JA (2003) Materials science: Enhancing drug function. *Science* 300:595–596.
9. Kim SC, *et al.* (2001) In vivo evaluation of polymeric micellar paclitaxel formulation: Toxicity and efficacy. *J Controlled Release* 72:191–202.
10. Kim T-Y, *et al.* (2004) Phase I and pharmacokinetic study of Genexol-PM, a cremophor-free, polymeric micelle-formulated paclitaxel, in patients with advanced malignancies. *Clin Cancer Res* 10:3708–3716.
11. Venne A, Li S, Mandeville R, Kabanov A, Alakhov V (1996) Hypersensitizing effect of Pluronic L61 on cytotoxic activity, transport, and subcellular distribution of Doxorubicin in multiple drug-resistant cells. *Cancer Res* 56:3626–3629.
12. Allen C, Yu Y, Eisenberg A, Maysinger D (1999) Cellular internalization of PCL_{20}-b-PEO_{44} block copolymer micelles. *Biochim Biophys Acta* 1421:32–38.
13. Luo L, Tam J, Maysinger D, Eisenberg A (2002) Cellular internalization of poly(ethylene oxide)-b-poly(ε-caprolactone) diblock copolymer micelles. *Bioconjugate Chem* 13:1259–1265.
14. Savic R, Luo L, Eisenberg A, Maysinger D (2003) Micellar nanocontainers distribute to defined cytoplasmic organelles. *Science* 300:615–618.
15. Moghimi SM, *et al.* (2004) Cellular distribution of nonionic micelles. *Science* 303:626–628.
16. Sengupta P, Holowka D, Baird B (2007) Fluorescence resonance energy transfer between lipid probes detects nanoscopic heterogeneity in the plasma membrane of live cells. *Biophys J* 92:3564–3574.
17. Li L, Wang H, Cheng J-X (2005) Quantitative coherent anti-Stokes Raman scattering imaging of lipid distribution in coexisting domains. *Biophys J* 89:3480–3490.
18. Matsumoto J, Nakada Y, Sakurai K, Nakamura T, Takahashi Y (1999) Preparation of nanoparticles consisted of poly(L-lactide)-poly(ethylene glycol)-poly(L-lactide) and their evaluation in vitro. *Int J Pharm* 185:93–101.
19. Ahmed F, Discher DE (2004) Self-porating polymersomes of PEG-PLA and PEG-PCL: Hydrolysis-triggered controlled release vesicles. *J Controlled Release* 96:37–53.
20. Steendam R, van Steenbergen MJ, Hennink WE, Frijlink HW, Lerk CF (2001) Effect of molecular weight and glass transition on relaxation and release behaviour of poly(DL-lactic acid) tablets. *J Controlled Release* 70:71–82.
21. Yamamoto Y, Yasugi K, Harada A, Nagasaki Y, Kataoka K (2002) Temperature-related change in the properties relevant to drug delivery of poly(ethylene glycol)-poly(D,L-lactide) block copolymer micelles in aqueous milieu. *J Controlled Release* 82:359–371.
22. McGuire WP, Rowinsky EK (1995) *Paclitaxel in Cancer Treatment* (Dekker, New York).
23. Zhang X, *et al.* (1997) An investigation of the antitumour activity and biodistribution of polymeric micellar paclitaxel. *Cancer Chemother Pharmacol* 40:81–86.
24. Huh KM, *et al.* (2005) Hydrotropic polymer micelle system for delivery of paclitaxel. *J Controlled Release* 101:59–68.
25. Balasubramanian SV, Straubinger RM (1994) Taxol-lipid interactions: Taxol-dependent effects on the physical properties of model membranes. *Biochemistry* 33:8941–8947.
26. Ali S, Minchey S, Janoff A, Mayhew E (2000) A differential scanning calorimetry study of phosphocholines mixed with paclitaxel and its bromoacylated taxanes. *Biophys J* 78:246–256.
27. Hamm-Alvarez SF, Sonee M, Loran-Goss K, Shen W-C (1996) Paclitaxel and nocodazole differentially alter endocytosis in cultured cells. *Pharm Res* 13:1647–1656.
28. Lin W-J, Juang L-W, Lin C-C (2003) Stability and release performance of a series of pegylated copolymeric micelles. *Pharm Res* 20:668–673.
29. Park EK, Lee SB, Lee YM (2005) Preparation and characterization of methoxy poly(ethylene glycol)/poly(ε-caprolactone) amphiphilic block copolymeric nanospheres for tumor-specific folate-mediated targeting of anticancer drugs. *Biomaterials* 26:1053–1061.
30. Maysinger D, Berezovska O, Savic R, Lim Soo P, Eisenberg A (2001) Block copolymers modify the internalization of micelle-incorporated probes into neural cells. *Biochim Biophys Acta* 1539:205–217.
31. Allen TM, Cullis PR (2004) Drug delivery systems: Entering the mainstream. *Science* 303:1818–1822.
32. Liaw J, Aoyagi T, Kataoka K, Sakurai Y, Okano T (1999) Permeation of PEO-PBLA-FITC polymeric micelles in aortic endothelial cells. *Pharm Res* 16:213–220.
33. Mahmud A, Lavasanifar A (2005) The effect of block copolymer structure on the internalization of polymeric micelles by human breast cancer cells. *Colloids Surf B Biointerfaces* 45:82–89.
34. Wang Y, Kausch CM, Chun M, Quirk RP, Mattice WL (1995) Exchange of chains between micelles of labeled polystyrene-block-poly(oxyethylene) as monitored by nonradiative singlet energy transfer. *Macromolecules* 28:904–911.
35. Haliloglu T, Bahar I, Erman B, Mattice WL (1996) Mechanisms of the exchange of diblock copolymers between micelles at dynamic equilibrium. *Macromolecules* 29:4764–4771.
36. Lentz BR (1994) Polymer-induced membrane fusion: Potential mechanism and relation to cell fusion events. *Chem Phys Lipids* 73:91–106.
37. Lee J, Lentz BR (1997) Evolution of lipidic structures during model membrane fusion and the relation of this process to cell membrane fusion. *Biochemistry* 36:6251–6259.
38. Arnold K, Zschoernig O, Barthel D, Herold W (1990) Exclusion of poly(ethylene glycol) from liposome surfaces. *Biochim Biophys Acta* 1022:303–310.
39. Boni LT, Stewart TP, Alderfer JL, Hui SW (1981) Lipid-polyethylene glycol interactions: II. Formation of defects in bilayers. *J Membr Biol* 62:71–77.
40. Tilcock CPS, Fisher D (1979) Interaction of phospholipid membranes with poly(ethylene glycol)s. *Biochim Biophys Acta* 557:53–61.
41. Aldwinckle TJ, Ahkong QF, Bangham AD, Fisher D, Lucy JA (1982) Effects of poly(ethylene glycol) on liposomes and erythrocytes: Permeability changes and membrane fusion. *Biochim Biophys Acta* 689:548–560.
42. Ahkong QF, Desmazes JP, Georgescauld D, Lucy JA (1987) Movements of fluorescent probes in the mechanism of cell fusion induced by poly(ethylene glycol). *J Cell Sci* 88:389–398.
43. Burt HM, Zhang X, Toleikis P, Embree L, Hunter WL (1999) Development of copolymers of poly(D,L-lactide) and methoxypolyethylene glycol as micellar carriers of paclitaxel. *Colloids Surf B Biointerfaces* 16:161–171.
44. Vasir JK, Reddy MK, Labhasetwar VD (2005) Nanosystems in drug targeting: Opportunities and challenges. *Curr Nanosci* 1:47–64.